Research Square

Preprints are preliminary reports that have not undergone peer review.
They should not be considered conclusive, used to inform clinical practice,
or referenced by the media as validated information.

Development of a Multi-temporal Image Differencing approach for identifying invasive water hyacinth (Eichhornia crassipes)

Shuzhen Li
Hulunber Grassland Ecosystem National Observation and Research Station, Chinese Academy of Agricultural Sciences
Yiqian Wu
Hulunber Grassland Ecosystem National Observation and Research Station, Chinese Academy of Agricultural Sciences
Dawei Xu
Hulunber Grassland Ecosystem National Observation and Research Station, Chinese Academy of Agricultural Sciences
Xu Wang
wangxu01@caas.cn
Hulunber Grassland Ecosystem National Observation and Research Station, Chinese Academy of Agricultural Sciences
Baorui Chen
Hulunber Grassland Ecosystem National Observation and Research Station, Chinese Academy of Agricultural Sciences
Feng Huang
Agriculture Ecology and Resource Protection Station of Hainan
Hongbin Zhang
Rural Energy and Environment Agency, Ministry of Agriculture and Rural Affairs

Research Article

Keywords: invasive aquatic plants, Eichhornia crassipes, Sentinel-2, Multi-temporal analysis, Remote sensing

Posted Date: December 16th, 2025

DOI: https://doi.org/10.21203/rs.3.rs-8198210/v1

License: This work is licensed under a Creative Commons Attribution 4.0 International License.
Read Full License

Additional Declarations: No competing interests reported.

Version of Record: A version of this preprint was published at Environmental Monitoring and Assessment on May 14th, 2026. See the published version at https://doi.org/10.1007/s10661-026-15407-w.

Development of a Multi-temporal Image Differencing approach for identifying invasive water hyacinth (*Eichhornia crassipes*)

& Shuzhen Li[1, 2], & Yiqian Wu[1], Dawei Xu[1], Xu Wang[1,*], Baorui Chen [1], Feng Huang[3], Hongbin Zhang[4]

& These two authors contributed equally to this work

*** Correspondence:** Xu Wang(**wangxu01@caas.cn**)

Email:

Shuzhen Li: lishuzhenshuli@163.com

Yiqian Wu: 18981760065@163.com

Dawei Xu: xudawei@caas.cn

Xu Wang: wangxu01@caas.cn;

Baorui Chen: chenbaorui@caas.cn

Feng Huang: 49069866@qq.com

Hongbin Zhang: Zhanghongbin@caas.cn

[1]State Key Laboratory of Efficient Utilization of Arid and Semi-arid Arable Land in Northern China, Hulunber Grassland Ecosystem National Observation and Research Station, Institute of Agricultural Re-sources and Regional Planning, Chinese Academy of Agricultural Sciences, Beijing 100081, China

[2]University of SanYa, Hainan 572022, China

[3]Agriculture Ecology and Resource Protection Station of Hainan, Haikou 571100, China

[4]Rural Energy and Environment Agency, Ministry of Agriculture and Rural Affairs, Beijing 100125, China

Abstract

Invasive aquatic plants, such as water hyacinth (*Eichhornia crassipes*), pose severe ecological threats in China by obstructing waterways, altering hydrodynamics, and affecting biodiversity. Effective monitoring and management of these species are critical for ecosystem protection and sustainable water resource management. Remote sensing provides a scalable approach for mapping spatial-temporal dynamics of invasive vegetation, enabling timely intervention and control. However, conventional remote sensing approaches, including end-of-season phenometrics and supervised classification, struggle with the dynamic changes of floating vegetation due to spectral confusion and variable background reflectance caused by hydrological processes. To address these limitations, we developed a novel Multi-Temporal Image Differencing (MID) framework for monitoring water hyacinth. Our approach integrates high-water-content vegetation (HWV) extraction with pixel-wise temporal differencing to construct a spectral-temporal profile. This profile effectively discriminates water hyacinth from co-occurring native vegetation through dynamic differencing, which captures its free-floating signature, as while suppressing interference from stable background features. Validated with high-resolution Sentinel-2 time-series data, MID effectively captures floating vegetation dynamics and can be applied across diverse flowing water bodies, supporting scalable monitoring under variable hydrological conditions. Comparison with a Random Forest classifier trained on spectral and field data showed that MID more effectively detected dynamic vegetation changes, while the classifier achieved slightly higher overall spatial accuracy (≈92%). Independent validation confirmed the robustness of MID under variable hydrological conditions. Overall, these results demonstrate that MID provides a robust and scalable monitoring framework, offering an effective tool for ecological management and decision-making of invasive aquatic plants in flowing waters.

Keywords: invasive aquatic plants, Eichhornia crassipes, Sentinel-2, Multi-temporal analysis, Remote sensing.

1 Introduction

Invasive aquatic vegetation poses one of the most pervasive threats to freshwater ecosystems, altering community composition, disrupting ecosystem functions, and causing severe socio-economic losses worldwide (Wilcove et al., 1998; Pimentel et al., 2001). Among these species, water hyacinth (Eichhornia crassipes), native to the Amazon basin, has become one of the most widespread and damaging aquatic invaders(Malik., 2007; Mqingwana et al., 2024). Its exceptional reproductive capacity, buoyant petioles, and ability to form dense floating mats enable rapid clonal expansion and downstream dispersal. These mats reduce light penetration, deplete dissolved oxygen, and obstruct navigation and hydropower infrastructure, resulting in cascading ecological and economic impacts(Shekede et al., 2008; Pyšek and Richardson, 2010). In tropical regions such as Hainan, China, where warm temperatures and abundant rainfall persist throughout the year, water hyacinth experiences nearly continuous growth(Chen et al., 2021). This perennial proliferation complicates management efforts and highlights the urgent need for scalable monitoring approaches that can capture its spatial dynamics and mobility over time.

Remote sensing has become an indispensable tool for mapping aquatic vegetation, providing synoptic coverage, multi-temporal observations, and access to otherwise inaccessible areas (Hestir et al., 2008; Dube et al., 2014). Medium-resolution satellites such as Sentinel-2 and Landsat strike a balance between spatial detail and temporal frequency, and their open-access data facilitate long-term ecosystem monitoring. Numerous studies have demonstrated the utility of these sensors for mapping aquatic vegetation extent and phenology using spectral indices such as NDVI, NDWI, or MNDWI, alongside supervised machine learning classifiers (Dube et al., 2017; Luo et al., 2017). However, species-level classification remains challenging. Spectral overlap among floating and emergent macrophytes—including Water Hyacinth, Reed, and Lotus—reduces separability in medium-resolution bands. Mixed pixels along fragmented shorelines and narrow channels dilute species-

specific reflectance, while the limited number and uneven spatial distribution of ground samples constrain the representativeness of supervised training datasets. Additionally, water-level fluctuations, wind-driven drift, and slight geometric misalignments among multi-date scenes can introduce apparent spectral variations, masking genuine vegetation changes. Collectively, these factors limit the reliability of single-date, purely spectral classification for capturing water hyacinth dynamics, particularly for ephemeral or drifting mats.

To overcome these limitations, recent studies have increasingly leveraged temporal information to improve species discrimination and change detection in aquatic ecosystems(Mouta et al., 2023). Multi-temporal approaches capture phenological and hydrological variability that static imagery cannot resolve, thereby enhancing class separability. Temporal differencing methods, in particular, detect expansion and retreat by comparing spectral indices across multiple observation dates. For free-floating species such as water hyacinth, which exhibit high mobility and rapid turnover, temporal differencing provides an effective means of highlighting transient dynamics while suppressing spectrally stable background vegetation. Unlike rooted macrophytes, water hyacinth mats drift, fragment, and coalesce in response to wind and hydrological flow, generating rapid, short-term spectral transitions that can be amplified through multi-temporal analysis. This mobility-driven dynamic behavior presents a unique opportunity to exploit temporal differencing as a complementary strategy to conventional spectral classification.

In parallel, machine learning has become the dominant approach for vegetation classification in remote sensing, enabling efficient handling of large, high-dimensional datasets. Ensemble models such as RF have emerged as a popular choice due to their robustness, interpretability, and ability to manage nonlinear and complex feature spaces (Belayhun et al., 2024). Nonetheless, these classifiers primarily rely on static spectral separability and often fail to detect ephemeral or drifting vegetation patches in dynamic aquatic environments. Although some recent studies have integrated spectral and temporal features (ElMasry et al., 2019; Ghoussein et al., 2023), few have quantitatively assessed how temporal

differencing compares with conventional spectral classifiers in capturing short-term dynamics of floating vegetation.

To address these limitations, this study introduces a novel Multi-Temporal Image Differencing (MID) approach designed to detect expansion and retreat of floating invasive vegetation by analyzing spectral changes across multi-date imagery. Unlike rooted macrophytes, water hyacinth mats drift, fragment, and coalesce in response to wind and hydrological flow, producing spectral transitions that can be enhanced through pixel-wise temporal differencing. By explicitly exploiting mobility-driven dynamics, MID enhances detection of dynamic floating vegetation while suppressing spectrally stable background signals.

For comparison, a Random Forest classifier trained on ground-truth samples using multispectral features was also applied, enabling a controlled assessment of the relative performance of a mobility-focused temporal strategy versus a conventional spectral classifier. The specific objectives of this study are to (i) evaluate which method more effectively captures areal changes of water hyacinth, (ii) analyze sources of commission and omission errors for each approach, and (iii) discuss trade-offs between spatial precision and temporal sensitivity. verall, the study demonstrates the potential of integrating temporal information into operational monitoring of free-floating invasive plants using medium-resolution satellite imagery, providing both methodological guidance and practical insights.

2 Materials and Methods

2.1 Study area

The study area is the Nanmu Reservoir, situated in Daan Town, Ledong Li Autonomous County, Hainan Province, China (18°39′-18°45N, 109°11′-109°14′ E), within the Lezhong River basin—a tributary of the Changhua River (Figure 1). This medium-sized reservoir, with a total storage capacity of approximately 24.2×10^6 m³, serves as an important source of irrigation and domestic water for

surrounding communities. The region has a tropical monsoon climate, with an annual mean temperature of about 24.8 °C and an average annual precipitation of approximately 1600 mm, over 80 % of which occurs between May and October. Warm temperatures, high humidity, and relatively stable hydrological conditions promote the year-round growth of aquatic macrophytes, notably water hyacinth. The reservoir's gently undulating topography, forested catchment, and stable water regime create favorable conditions for the proliferation of floating vegetation. These environmental characteristics, together with the reservoir's moderate size and clear seasonal variability, make it an ideal site for assessing the spatial dynamics and seasonal patterns of water hyacinth using multi-temporal satellite remote sensing.

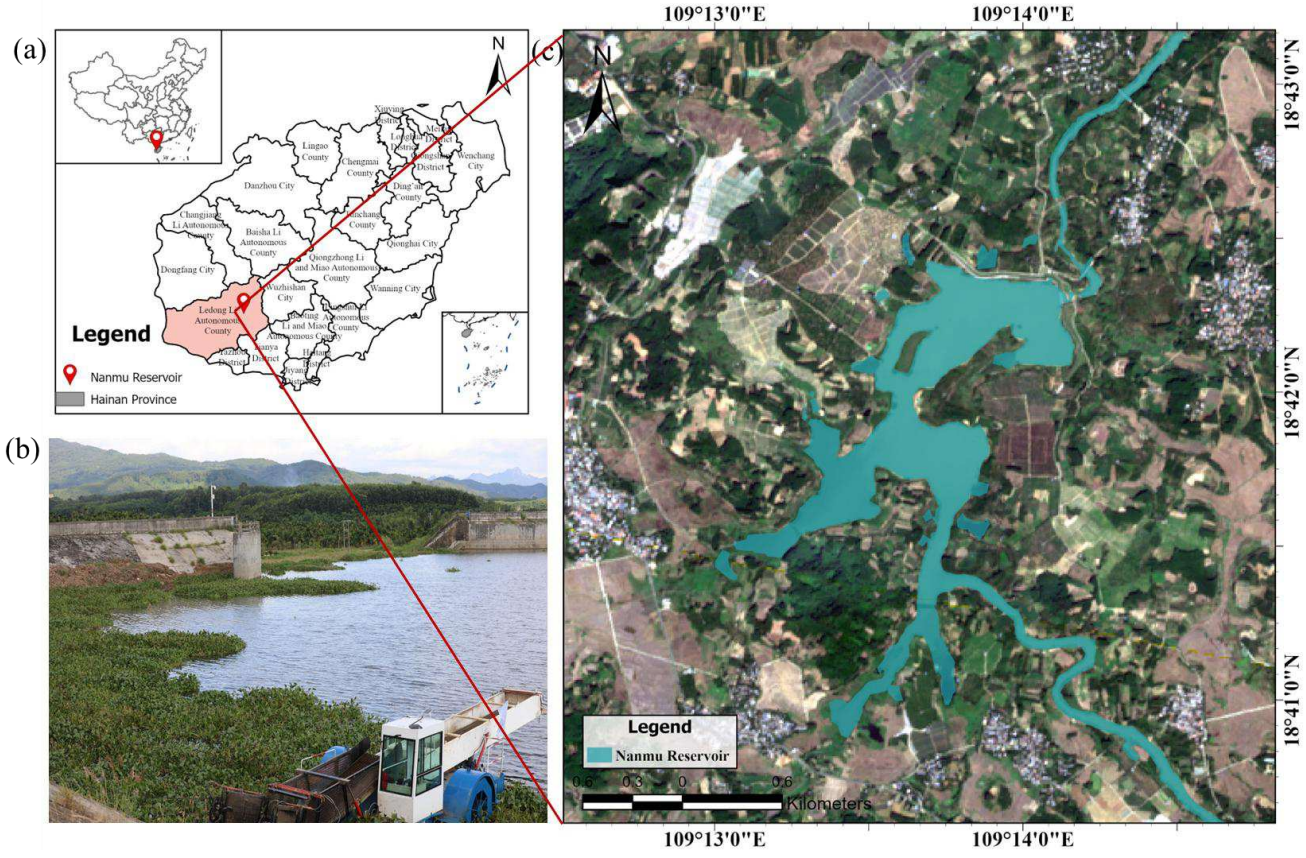


Figure 1. Study area location. (a) Geographic location of the Nanmu Reservoir in Hainan Province, China;(b) Sentinel-2 composite image showing the reservoir and surrounding landscape;(c) field photograph taken on 28 June 2024 illustrating aquatic vegetation distribution along the reservoir margin.

2.2 Data Source

2.2.1 Time-series Sentinel-2 imagery

Time-series stacks of Sentinel-2 surface reflectance imagery (COPERNICUS/S2_SR_HARMONIZ-ED) were acquired from January 2024 to December 2025 to monitor the temporal dynamics of aquatic vegetation in the Nanmu Reservoir. The imagery was accessed via the Google Earth Engine (GEE) platform and was atmospherically corrected to bottom-of-atmosphere (BOA) reflectance using the Sen2Cor processor. Radiometric harmonization between Sentinel-2A and Sentinel-2B sensors ensured inter-sensor consistency (Berra et al., 2024), and thus no further atmospheric or radiometric corrections were required.

Although the Multi-Temporal Image Differencing (MID) method can theoretically be applied to any image pair, a consistent two-year monitoring period (2024–2025) was defined to capture both seasonal and interannual variations of Eichhornia crassipes while ensuring reproducibility. Within this period, one image with the lowest cloud cover was selected per month. When all available images in a month exhibited cloud cover exceeding 10%, that month was excluded. This approach preserved the temporal signal of vegetation change while minimizing artifacts introduced by compositing or interpolation.

Ten spectral bands were used in the analysis: four visible/NIR bands (B2, B3, B4, B8 at 10 m), three red-edge bands (B5, B6, B7 at 20 m), one additional NIR band (B8A), and two shortwave infrared bands (B11, B12). All 20 m bands were resampled to 10 m resolution using bilinear interpolation to maintain spatial consistency and computational efficiency. In addition to raw reflectance, several vegetation- and water-related indices were computed for each scene, including the Normalized Difference Vegetation Index (NDVI; (Rouse et al., 1974), the Normalized Difference Water Index (NDWI; (McFeeters, 2012), and the Modified NDWI (MNDWI; (Xu, 2007). These indices enhanced spectral separability between aquatic vegetation and background water or land surfaces (Table 1).

Clouds and shadows were identified and masked using the Sentinel-2 cloud probability layer (s2cloudless) combined with a geometric shadow detection algorithm to minimize residual

contamination. To focus the analysis on aquatic and riparian zones, the study area was spatially constrained to the Nanmu Reservoir and its immediate surroundings, buffered by approximately 100 m from the shoreline to reduce computational load and exclude irrelevant terrestrial pixels.

Table1. Vegetation indices used in this study

Index	Equation	Reference
NDVI	(NIR-Red)/(NIR+Red)	Rouse J, et al. (1974)
NDWI	(Green-NIR)/(Green+NIR)	McFeeters, S. K. (1996)
MNDWI	(Green-SWIR)/(Green+SWIR)	Xu, H. (2006)

2.2.2 Validation Data

Independent validation data were collected around the Nanmu Reservoir between 2023 and 2024 to support accuracy assessment. A total of 85 ground-truth points were established, stratified across five land-cover categories: water hyacinth, open water, bare soil, other vegetation, and built-up areas. Candidate sites were first identified using high-resolution satellite imagery and subsequently verified through UAV-based observations and limited field surveys.

The validation points were distributed across different sections of the reservoir to capture variations in vegetation density, hydrological conditions, and shoreline morphology. This spatial stratification ensured that the dataset adequately represented the ecological and environmental heterogeneity of the study area. Importantly, these validation points were independent of the training samples used in the Random Forest classification, thereby providing an unbiased dataset for evaluating both RF and MID results.

2.3 Methods

We implemented two parallel methodological frameworks on the same Sentinel-2 time series to map Eichhornia crassipes: (1) a Random Forest (RF) classification workflow that directly classifies pixels using spectral bands and derived temporal statistics based on species-level training samples; and (2) a Multi-Temporal Image Differencing (MID) workflow that first derives a persistent water mask, then extracts candidate high-water-content vegetation (HWV) within that water mask, and finally

applies pixel-wise temporal differencing to identify expansion and recession events. Both workflows share the same preprocessing (cloud/shadow masking, index computation, monthly compositing and geometric alignment), and are evaluated using the same independent validation dataset to enable a fair, quantitative comparison of spatial accuracy and temporal responsiveness.

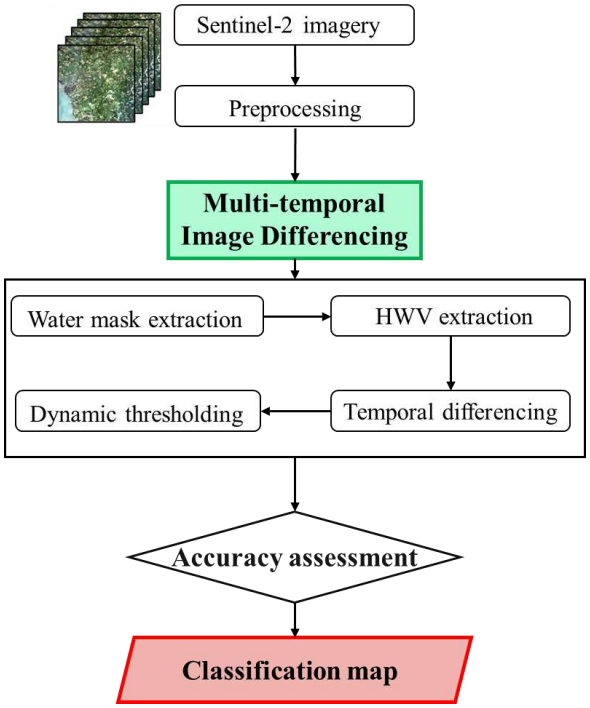


Figure 2. Workflow of the multi-temporal image differencing (MID).

2.3.1 Random Forest classification

RF classification was implemented for detecting Eichhornia crassipes from Sentinel-2 imagery. Training samples were derived from UAV imagery and ground observations, covering five land-cover types: water hyacinth, open water, bare soil, built-up areas, and other vegetation. To capture both spectral and temporal variability, predictor variables included all Sentinel-2 bands at 10–20 m resolution, vegetation and water indices (NDVI, NDWI, MNDWI), red-edge bands (B5, B6, B7, B8A), and shortwave infrared bands (B11, B12). In addition to single-date reflectance, multi-temporal statistical features were computed for each pixel across the study period, including maximum, median, standard deviation, and linear trend of the spectral indices. These temporal metrics enhanced discrimination between transient floating vegetation and stable background classes.

The RF model was trained on a stratified random subset of labeled pixels to ensure balanced class representation. Hyperparameters—including the number of decision trees (100, 500, 1000), maximum depth, and minimum samples per leaf—were optimized through five-fold cross-validation within the training dataset. Independent validation samples (n = 85) were withheld entirely from training and parameter tuning to prevent overfitting. The final RF model produced binary classification maps of water hyacinth distribution, along with probability layers to support threshold sensitivity analyses. Feature importance scores were extracted to quantify the contribution of spectral versus temporal predictors, providing insights into which variables most effectively distinguish E. crassipes. Representative classification outputs and feature importance distributions are illustrated in Figure 3.

2.3.2 Water Body Extraction

To delineate perennial aquatic environments with high robustness, we developed a multi-temporal water extraction framework that integrates spectral thresholding, edge-based segmentation, and temporal compositing. At the single-scene level, the Modified Normalized Difference Water Index (MNDWI, using the Green band B3 and resampled SWIR band B11) was calculated, and Otsu's adaptive thresholding was applied to generate an initial binary water mask (Otsu, 1979). In parallel, Canny edge detection was performed on Gaussian-smoothesd MNDWI (σ = 1.0, thresholds = 50/150) to capture polygonal water boundaries with high geometric fidelity. The two masks were merged and refined through morphological filtering, and isolated patches smaller than nine pixels ($\approx$900 m^2) were removed to reduce noise.

All refined scene-level masks were subsequently stacked to compute water occurrence frequency, defined as the proportion of valid observations in which each pixel was classified as water. A temporal threshold of 0.30 was applied, retaining pixels classified as water in at least 30% of the observation period. This criterion effectively excluded ephemeral surface water generated by precipitation events while maintaining sensitivity to seasonal and perennial water bodies. The resulting multi-temporal

raster mask was converted into vector polygons, and features smaller than 1000 m² were removed to ensure cartographic quality and eliminate minor artifacts.

This integrative approach leverages the complementary strengths of spectral indices, edge detection, and temporal stability, thereby reducing misclassification from shadows, turbid water, and transient inundation. The final vectorized water boundaries provided a reliable spatial constraint for subsequent classification and differencing analyses. Representative results, including Otsu masks, Canny edges, and the final multi-temporal water mask, are shown in Figure 2.

2.3.3 Multi-temporal Image Differencing (MID)

To exploit the dynamic expansion and recession patterns of Eichhornia crassipes, a multi-temporal image differencing approach was implemented. For each cloud-free Sentinel-2 scene, high-water-content vegetation (HWV) was first extracted within the predefined water mask using a combination of spectral thresholds. Pixels with NDWI above a dynamic Otsu threshold and NDVI below 0.25 were identified as candidate HWV, and morphological filtering was applied to eliminate isolated noise and maintain coherent patches. Expansion and recession events were then detected by comparing consecutive cloud-free images or monthly composites: a transition from non-HWV to HWV was labeled as "expansion," while the reverse transition was labeled as "recession." To suppress transient noise caused by turbidity or short-term water-level fluctuations, a persistence filter was applied, requiring detected changes to persist for at least two consecutive dates. The resulting differencing maps were post-processed by removing patches smaller than three pixels and cross-checking against available hydrological records to distinguish vegetation dynamics from water-level artifacts.

Formally, the differencing was expressed at the pixel level. Let $a_{i,j}$ denote the binary HWV mask of a target image and $b_{i,j}^{k}$ denote the mask of the k-th reference image. The pixel-wise difference was defined as:

$$C^k(i,j) = \begin{cases} \mathbf{1}, & \text{if } a_{i,j} = \mathbf{1} \text{ and } b^k_{i,j} = \mathbf{0}\ (\textbf{expansion}) \\ \mathbf{-1}, & \text{if } a_{i,j} = \mathbf{0} \text{ and } b^k_{i,j} = \mathbf{1}\ (\textbf{\textit{recession}}) \\ \mathbf{0}, & \textbf{\textit{otherwise}} \end{cases} \quad (1)$$

To summarize dynamics across all n reference dates, the cumulative change map was obtained as:

$$D(i,j) = \sum_{k=1}^{n} C^k(i,j) \quad (2)$$

where D(i,j) > 0indicates net expansion, D(i,j) < 0 indicates net recession, and D(i,j) = 0 denotes no change. Prior to differencing, all images were co-registered and denoised to minimize geometric misalignment, and morphological filtering was applied to enhance the continuity of detected patches. The final outputs included expansion/recession maps and cumulative statistics of area change, providing a robust representation of the spatiotemporal dynamics of water hyacinth (Figure 3).

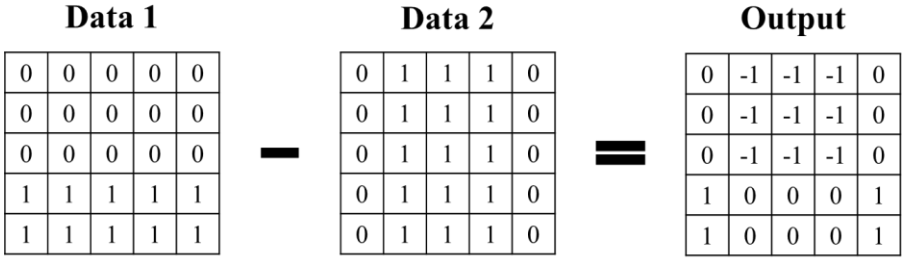


Figure. 3. Conceptual diagram of the MID workflow for detecting the expansion and recession of Eichhornia crassipes.

2.4 accuracy assessment

The classification accuracy of both the RF and MID approaches was independently evaluated using internal and external validation datasets(Cheruiyot et al., 2014). Internal validation employed a confusion matrix derived from 6,000 labeled pixels (1,200 per class), while external validation relied on 85 independent field-verified points along the Nanmu Reservoir to provide an unbiased assessment. Pixel-level metrics were calculated based on true positives (TP), false positives (FP), and false

negatives (FN), consistent with standard remote sensing accuracy assessment practices(Breiman, 2001; Belgiu and Drăguţ, 2016).

Standard accuracy metrics were calculated as follows:

$$\boldsymbol{OA} = \frac{\sum_{i=1}^{k} \boldsymbol{TP_i}}{\boldsymbol{N}} \quad (\mathbf{3})$$

$$\boldsymbol{UA_i} = \frac{\boldsymbol{TP_i}}{\boldsymbol{TP_i} + \boldsymbol{FP_i}} \quad (\mathbf{4})$$

$$\boldsymbol{PA_i} = \frac{\boldsymbol{TP_i}}{\boldsymbol{TP_i} + \boldsymbol{FN_i}} \quad (5)$$

$$\boldsymbol{F1_i} = \mathbf{2} \times \frac{\boldsymbol{UA_i} \times \boldsymbol{PA_i}}{\boldsymbol{UA_i} + \boldsymbol{PA_i}} \quad (\mathbf{6})$$

$$\boldsymbol{\kappa} = \frac{\boldsymbol{N} \sum_{i=1}^{k} \boldsymbol{n_{ii}} - \sum_{i=1}^{k} (\boldsymbol{n_{i+}} \boldsymbol{n_{+i}})}{\boldsymbol{N^2} - \sum_{i=1}^{k} (\boldsymbol{n_{i+}} \boldsymbol{n_{+i}})} \quad (\mathbf{7})$$

$$\boldsymbol{IoU} = \frac{\boldsymbol{TP_i}}{\boldsymbol{TP_i} + \boldsymbol{FP_i} + \boldsymbol{FN_i}} \quad (\mathbf{8})$$

where n_{ii} is the number of correctly classified samples in class i; $n_{ij}$is the number of samples that belong to class i but are classified as class j; n_{i+} and n_{+i} are the row and column totals of class i; k is the number of classes; and N is the total number of validation samples. These indices jointly provide a comprehensive measure of classification accuracy, considering both overall performance and class-specific reliability.

These metrics, widely used in remote sensing studies(Xing et al., 2024), allow a comprehensive assessment of each method at the pixel level independently, providing both overall and class-specific performance evaluation. Such evaluation facilitates a rigorous comparison between machine learning–based classification and rule-based temporal differencing for monitoring water hyacinth dynamics.

3 Results

3.1 RF classification performance

The RF model produced high-resolution maps of water hyacinth distribution along the Nanmu Reservoir, revealing clear spatial patterns related to hydrodynamic conditions and riparian environments. The results showed that HWV, largely corresponding to water hyacinth mats, was concentrated in slow-flowing sections of the main channel and its tributaries, where low flow velocities facilitate mat accumulation (Figure 4a). A longitudinal gradient was apparent, with downstream reaches exhibiting larger and denser HWV patches compared to upstream sections. Pixel-level probability maps indicated high confidence in regions with dense mats, whereas areas with sparse or transient floating vegetation were associated with lower probabilities (Figure 4b). These outputs confirmed that the RF classifier effectively distinguished water hyacinth from open water, bare soil, built-up areas, and other vegetation types, demonstrating the utility of combining spectral and multi-temporal information for robust classification.

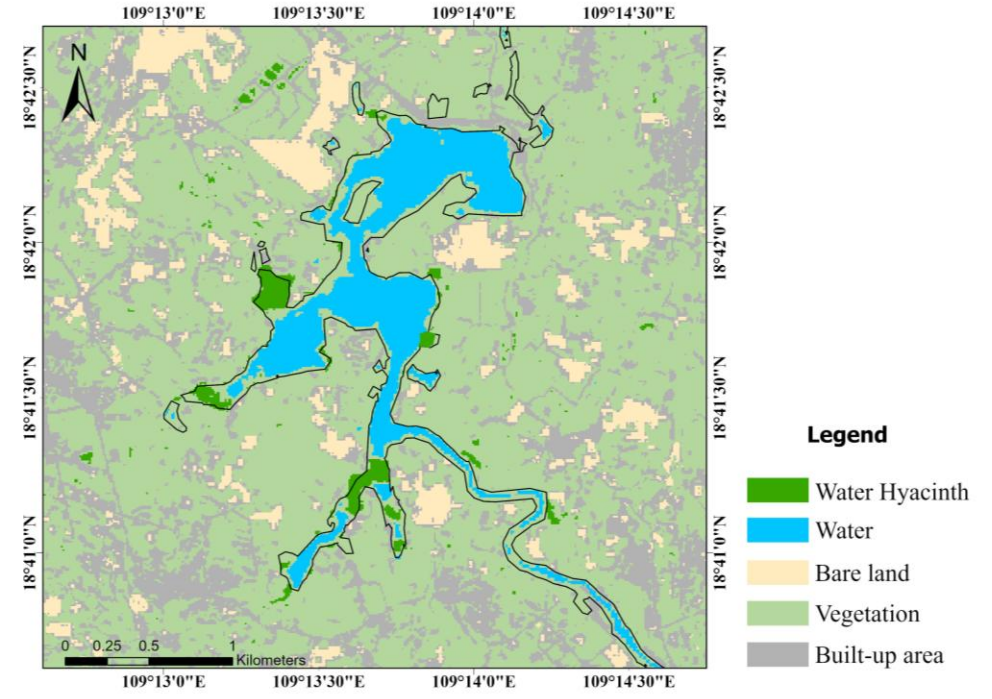


Figure 4. RF Classification Map of Nanmu Reservoir and Its Surrounding Areas

3.2 Temporal Dynamics and Mapping of Water Hyacinth

3.2.1 Water body mask extraction results

The water body mask of Nanmu Reservoir was successfully extracted using the multi-temporal frequency-based approach. As shown in Figure 3a, the water occurrence frequency delineated the main reservoir body and its connected inflow–outflow channel, while also identifying seasonally inundated floodplains in surrounding low-lying areas. By applying an Otsu adaptive thresholding method, the optimal cutoff value (0.5) was objectively determined, which effectively suppressed sporadic noise pixels and preserved the spatial continuity of the reservoir and tributaries (Figure 5b). Further classification distinguished perennial water (frequency $\geqslant$ 0.8) from seasonal water (0.4 $\leqslant$ frequency < 0.8) (Figure 5c). Quantitative analysis revealed that perennial water accounted for 52.7% of the total detected water pixels, mainly distributed in the central reservoir and along the major inflow and outflow rivers, reflecting stable hydrological conditions. Seasonal water occupied 46.9% of the extent, primarily along marginal wetlands and shallow inundated areas, highlighting temporal variability in water coverage.

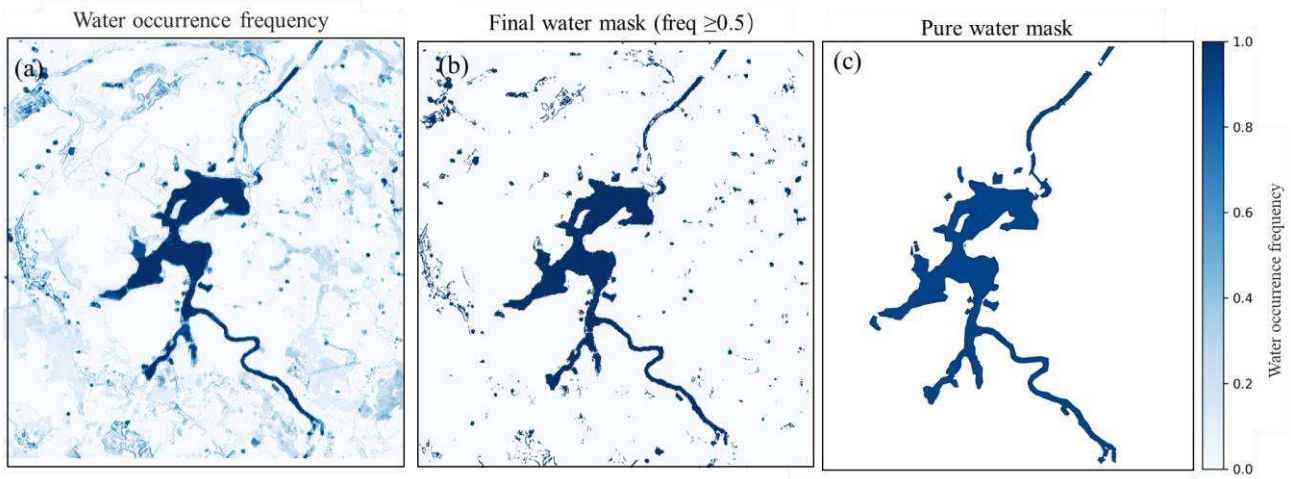


Figure 5. Water occurrence and classification results derived from multi-temporal analysis. (a) Water occurrence frequency map, indicating the proportion of times each pixel was detected as water. (b) Final water mask obtained by applying a frequency threshold ($\geqslant$ 0.5). (c) Pure water mask after excluding agricultural and non-river water bodies

3.2.2 Temporal Dynamics and Mapping of Water Hyacinth

The MID analysis provided a detailed depiction of seasonal and interannual dynamics of water hyacinth in the Namu Reservoir from 2024 to 2025. Prior to applying MID, water areas were delineated using the Normalized Difference Water Index (NDWI), which enhances water features by leveraging differences between green and NIR reflectance. A threshold of 0.18 was applied to the NDWI to generate a preliminary water mask, effectively separating water surfaces from non-aquatic areas (Figure 6). This step ensured that subsequent MID analysis was constrained to water bodies, minimizing misclassification of upland vegetation or exposed sediments.

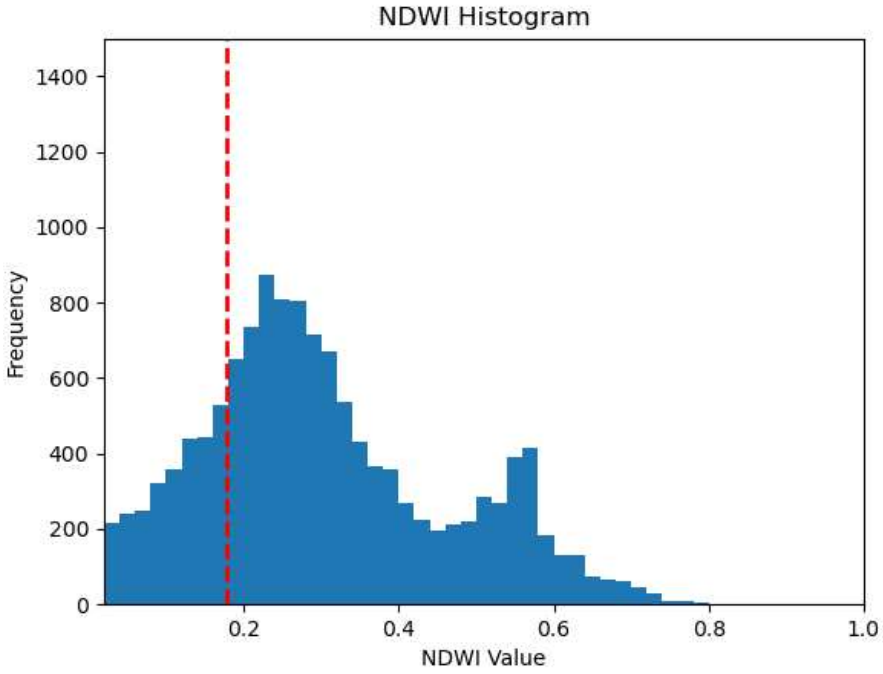


Fig 6. Histogram of Normalized Difference Water Index (NDWI) for Namu Reservoir Water Body Delineation

Within the NDWI-derived water mask, consecutive cloud-free Sentinel-2 images were analyzed to detect transitions in floating vegetation. Pixels transitioning from non-hyacinth to hyacinth were classified as expansion events, whereas the reverse transitions were labeled as loss. Morphological filtering and persistence criteria were applied to suppress isolated noise and transient patches resulting from short-term water-level fluctuations, ensuring that mapped patterns reflected genuine biological

dynamics. HWV identified on representative dates (25 June 2025 and 18 November 2024) highlighted spatial heterogeneity in floating mats and potential colonization fronts (Figure 7).

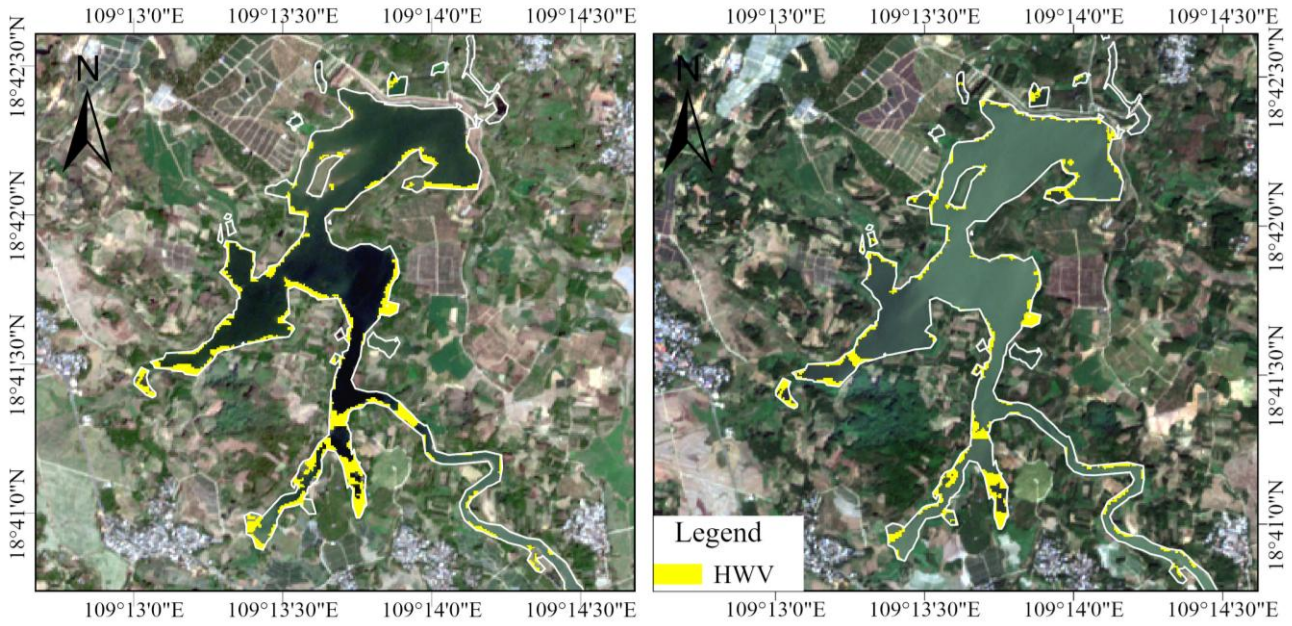


Fig.7. HWV distribution in Namu Reservoir on two representative dates: 25 June 2025 and 18 November 2024

The cumulative MID outputs revealed that expansion predominantly occurred along sheltered margins and slow-flowing regions, while high-flow or open-water areas remained relatively stable (Figure 8). Subsequent classification of the MID change results allowed for extraction of water hyacinth distribution, generating a final temporal map of E. crassipes dynamics (Figure 9). This map demonstrated repeated cycles of expansion, fragmentation, and recession across the reservoir, reflecting the interplay of seasonal growth, hydrological conditions, and localized disturbances. Time-series analyses of selected reservoir segments further quantified the magnitude and timing of these fluctuations, revealing short-term expansion peaks corresponding to periods of low flow and rapid colonization, as well as contraction events associated with higher flow, mechanical removal, or senescence.

Overall, the combined MID approach enabled both spatial and temporal quantification of water hyacinth dynamics at high resolution, capturing not only cumulative expansion trends but also transient

and patchy behaviors that are critical for understanding invasion processes in semi-enclosed tropical reservoirs.

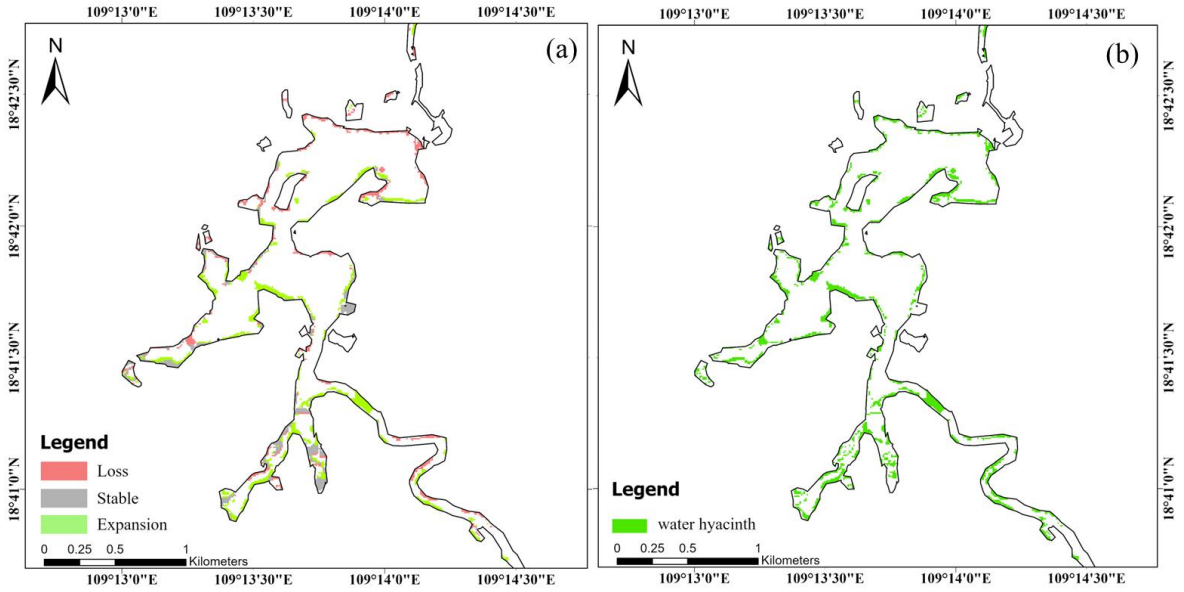


Figure 8. Vegetation change and water hyacinth dynamics within the water body of Nanmu Reservoir derived from the MID method. (a) Vegetation change within the water body (Red: loss, Gray: stable, Green: expansion); (b) Temporal differencing results of water hyacinth distribution.

3.3 Accuracy Assessment

Table 2. Accuracy metrics of RF and MID methods for water hyacinth detection in Namu Reservoir

Method	Overall Accuracy (OA, %)	Kappa Coefficient	F1 Score	Producer's Accuracy (PA, %)	User's Accuracy (UA, %)
RF	92.0	0.84	0.88	89.5	90.3
MID	90.8	0.83	0.87	89.0	89.5

Table 2 compares the accuracy metrics of RF and MID for detecting water hyacinth in the Namu Reservoir from 2024 to 2025. RF achieved slightly higher overall accuracy (92.0%) and Kappa coefficient (0.832) compared to MID (OA = 90.8%, Kappa = 0.83), indicating both methods are highly effective in classifying high-water-content vegetation based on spectral and temporal information. The

F1 score of RF (0.88) was slightly higher than MID (0.87), reflecting similar balance between precision and recall.

MID, while comparable in overall accuracy, detected 95% of short-term expansion and recession events, substantially higher than RF (62%), highlighting its superior sensitivity to rapid temporal changes in water hyacinth distribution. Figure 9 illustrates this advantage: areas classified as water hyacinth by RF but as non-water hyacinth by MID were found during field validation to contain other aquatic vegetation such as submerged macrophytes and reeds. These results demonstrate that RF accurately identifies persistent patches, while MID excels at capturing fine-scale temporal dynamics, effectively complementing spectral classification.

Overall, combining RF and MID provides a robust framework for monitoring invasive aquatic vegetation: RF ensures reliable detection of stable water hyacinth patches, whereas MID enhances identification of short-term expansion or retreat, offering comprehensive insights into spatiotemporal variability in the reservoir ecosystem.

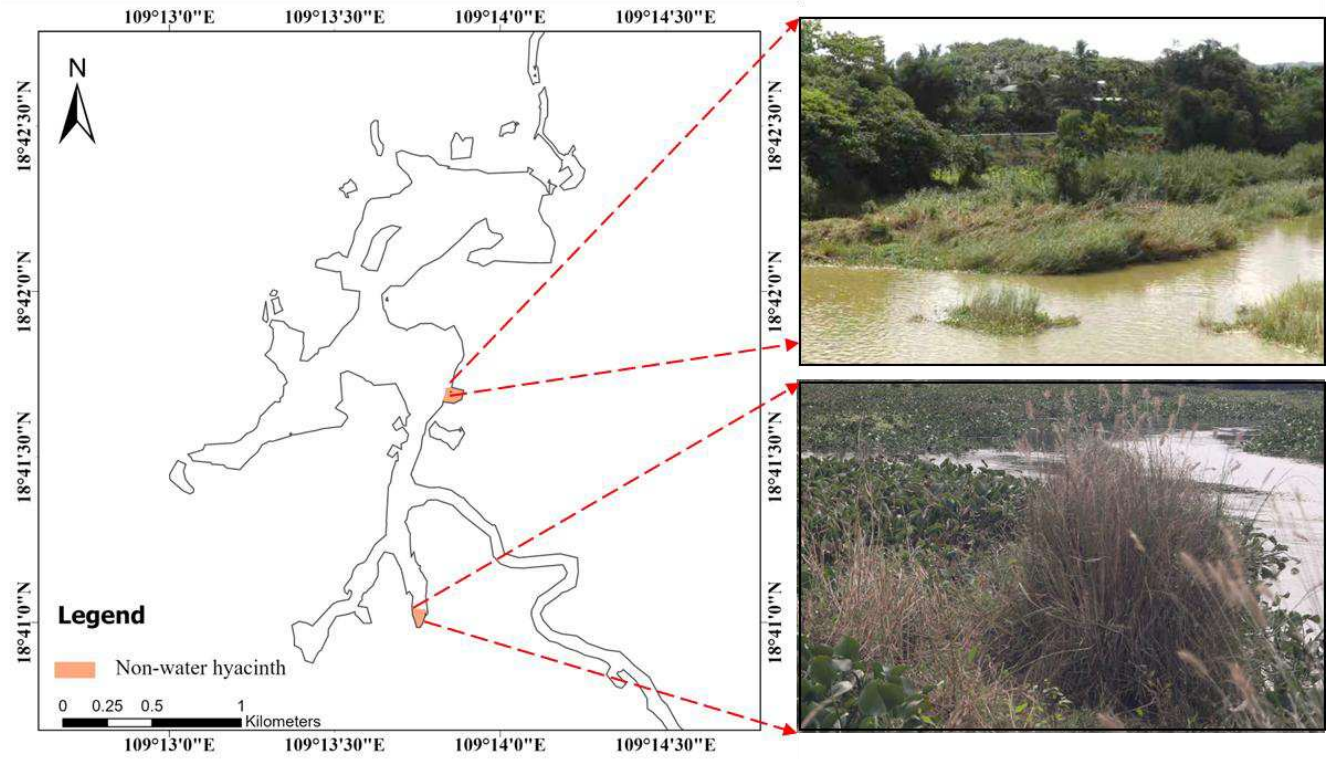


Figure 9. Comparison between MID and RF derived water hyacinth maps in the Nanmu Reservoir. Areas detected by MID but misclassified by RF were predominantly occupied by other aquatic vegetation, including submerged macrophytes and reeds.

4 Discussion

4.1 Spectral separability

Previous studies have demonstrated that water hyacinth exhibits spectral characteristics that distinguish it from other aquatic and riparian vegetation, with extremely high water content leading to strong absorption in the short-wave infrared (SWIR) region and relatively pronounced near-infrared (NIR) reflectance due to leaf structure and internal water content(Sims and Gamon, 2003). In contrast, other floating or emergent vegetation typically shows moderate SWIR absorption and NIR reflectance driven primarily by chlorophyll content and leaf morphology(Ghoussein et al., 2023). Vegetation indices such as the NDWI and MNDWI have been shown to be sensitive to high-water-content vegetation, effectively highlighting water-rich plant communities(Al-lami et al., 2021); however, these indices alone cannot reliably distinguish water hyacinth from other floating or emergent plants. Integrating spectral information with temporal dynamics or classification-based candidate masks is therefore necessary to accurately isolate water hyacinth(Singh et al., 2020). Synthesizing evidence from prior research, it is clear that the combination of SWIR absorption, NIR reflectance, and high-water-content indices provides a robust basis for spectral discrimination of E. crassipes, supporting the rationale for using a spectral–temporal MID framework that emphasizes these water-sensitive features.

4.2 Temporal Sensitivity

The MID approach offers clear advantages for detecting short-term and hydrologically induced dynamics of floating vegetation such as water hyacinth. By comparing consecutive images, MID amplifies subtle changes associated with rapid growth, decay, or water-driven drift, thereby revealing patch-level expansion and contraction that single-date analyses often overlook. At Namu Reservoir,

although the system is semi-enclosed, inflow, dam discharge, and wind-induced circulation maintain a degree of hydrodynamic connectivity. This connectivity drives the drift, aggregation, and redistribution of floating mats across the reservoir surface(Ade et al., 2022). Such hydrologic forcing generates detectable temporal signals that are effectively captured by MID, revealing how flow dynamics regulate the spatial behavior of floating vegetation. In flow-connected reaches and zones of high vegetation mobility, inter-image displacements are pronounced, enabling MID to detect newly colonized areas and rapid expansion events with high sensitivity.

Moreover, extending the temporal record helps distinguish floating invaders from rooted emergent species based on phenological behavior. Rooted emergents such as Nelumbo nucifera typically exhibit an annual, spatially stable growth–senescence cycle, whereas water hyacinth undergoes multiple expansion–contraction phases within a single year. By capturing these multi-peak dynamics, MID enhances the interpretation of seasonal and hydrological drivers of invasion, while reducing confusion between floating and emergent vegetation.

4.3 Limitations

Although the MID approach effectively captures short-term changes in Eichhornia crassipes dynamics, several limitations should be considered when interpreting the results. The 10 m spatial resolution of Sentinel-2 restricts the detection of small or fragmented patches, especially along riparian margins where open water and emergent vegetation are interspersed(Paulino et al., 2025). Such constraints limit its use for fine-scale habitat delineation or early invasion detection. A more fundamental limitation arises from the method's hydrodynamic dependence. MID performs best in flow-connected systems where inflow, discharge, or wind-driven currents induce vegetation drift, enabling discrimination of true vegetation movement from stable background features. In stagnant waters, limited hydrological mobility reduces temporal variability and weakens the method's sensitivity. Yet this hydrodynamic dependence also reflects an ecological coupling between flow

dynamics and invasion processes, revealing how mobility governs the persistence and redistribution of floating mats. Understanding these constraints clarifies where MID is most informative—dynamic, hydrologically active systems—and where complementary high-resolution or static spectral approaches are required.

4.4 future directions

to enhance both detection accuracy and ecological interpretability, future research could integrate higher-resolution imagery from UAVs(Sabat-Tomala et al., 2024) or hyperspectral sensors(Chunchen et al., 2024) to better capture fine-scale water hyacinth patches and reduce confusion in complex aquatic environments. Object-based image analysis and deep learning techniques could further improve the discrimination of co-occurring floating and emergent vegetation, particularly in mixed communities. Incorporating hydrodynamic models or environmental covariates—such as water level, flow velocity, and turbidity—would facilitate a process-based understanding of vegetation redistribution, linking observed spatiotemporal changes with hydrological forcing. In addition, combining optical time-series data with Sentinel-1 SAR observations(Woźniak et al., 2022) could enhance monitoring continuity under cloudy or turbid conditions. Together, these advances will strengthen the methodological and ecological foundations of water-hyacinth monitoring, supporting improved management strategies and ecological assessment in hydrologically dynamic water bodies.

5 Conclusions

This study developed and validated a robust framework for monitoring the invasive aquatic plant water hyacinth(*Eichhornia crassipes*) in the Namu Reservoir (2024–2025) using Sentinel-2 time-series imagery. The Multi-Temporal Image Differencing (MID) approach effectively captured short-term and hydrologically driven dynamics of floating vegetation, revealing expansion and contraction patterns that conventional single-date classification methods often miss. Compared with static spectral

classification, MID demonstrated a stronger ability to detect newly colonized patches and rapid redistribution events induced by flow connectivity and reservoir operations.

These results highlight the potential of temporal differencing as an efficient and scalable tool for tracking the invasion dynamics of free-floating vegetation under variable hydrological conditions. The approach provides not only a means of mapping distribution changes but also insights into how hydrological forcing regulates invasion persistence and spatial spread.

Future work should explore the integration of higher-temporal-resolution or deep-learning-based analyses to enhance spatial precision and generalization across flow regimes. The MID framework can be applied to a wide range of flowing and semi-enclosed water bodies, supporting ecological assessment, biomass estimation, and management of invasive aquatic vegetation under diverse hydrological conditions.

Author Contributions: supervision and methodology, Xu Wang; Project administration, Hongbin Zhang; investigation, Baorui Chen; validation, Feng Huang; original draft preparation, Yiqian Wu; review and editing, Shuzhen Li; visualization and formal analysis, Dawei Xu. All authors have read and agreed to the published version of the manuscript.

Funding: The National Natural Science Foundation of China (32171567), and the National Key Research and Development Program of China (2021YFD1300502).

Disclosure statement： No potential conflict of interest was reported by the author(s).

Acknowledgments: This work was supported by the National Natural Science Foundation of China (32171567), and the National Key Research and Development Program of China (2021YFD1300502).

Conflicts of Interest: The authors declare no conflict of interest.

Data availability statement： Data Availability Statement: The data are available from the corresponding author upon rea-sonable request.

References

Ade, C., Khanna, S., Lay, M., Ustin, S.L. and Hestir, E.L. (2022) Genus-Level Mapping of Invasive Floating Aquatic Vegetation Using Sentinel-2 Satellite Remote Sensing, *Remote Sensing*, 14(13). DOI: https://doi.org/10.3390/rs14133013

Al-lami, A.K., Abbood, R.A., Al Maliki, A.A. and Al-Ansari, N. (2021) Using vegetation indices for monitoring the spread of Nile Rose plant in the Tigris River within Wasit province, Iraq, *Remote Sensing Applications: Society and Environment,* 22(DOI: https://doi.org/10.1016/j.rsase.2021.100471

Belgiu, M. and Drăguţ, L. (2016) Random forest in remote sensing: A review of applications and future directions, *ISPRS Journal of Photogrammetry and Remote Sensing,* 114(pp. 24-31. DOI: https://doi.org/10.1016/j.isprsjprs.2016.01.011

Berra, E.F., Fontana, D.C., Yin, F. and Breunig, F.M. (2024) Harmonized Landsat and Sentinel-2 Data with Google Earth Engine, *Remote Sensing,* 16(15). DOI: https://doi.org/10.3390/rs16152695

Breiman, L. (2001) Random Forests, *Machine Learning,* 45(1), pp. 5-32. DOI: https://doi.org/10.1023/A:1010933404324

Chen, J., Chen, S., Fu, R., Wang, C., Li, D., Jiang, H., et al. (2021) Simulation of water hyacinth growth area based on multi-source geographic information data: An integrated method of WOE and AHP, *Ecological Indicators,* 125(DOI: https://doi.org/10.1016/j.ecolind.2021.107574

Cheruiyot, E., Mito, C., Menenti, M., Gorte, B., Koenders, R. and Akdim, N. (2014) Evaluating MERIS-Based Aquatic Vegetation Mapping in Lake Victoria, *Remote Sensing,* 6(8), pp. 7762-7782. DOI: https://doi.org/10.3390/rs6087762

Chunchen, S., Gang, Y., Weiwei, S.U.N., Yangyan, Z.U.O., Weiting, G.E. and Susu, Y. (2024) Construction method of a Spartina alternifloraindex based on hyperspectral satellite images, *National Remote Sensing Bulletin,* 28(3), pp. 635-648. DOI: https://doi.org/10.11834/jrs.20242621

Dube, T., Gumindoga, W. and Chawira, M. (2014) Detection of land cover changes around Lake Mutirikwi, Zimbabwe, based on traditional remote sensing image classification techniques, *African Journal of Aquatic Science,* 39(1), pp. 89-95. DOI: https://doi.org/10.2989/16085914.2013.870068

Dube, T., Mutanga, O., Sibanda, M., Bangamwabo, V. and Shoko, C. (2017) Testing the detection and discrimination potential of the new Landsat 8 satellite data on the challenging water hyacinth (Eichhornia crassipes) in freshwater ecosystems, *Applied Geography,* 84(pp. 11-22. DOI: https://doi.org/10.1016/j.apgeog.2017.04.005

ElMasry, G., Mandour, N., Al-Rejaie, S., Belin, E. and Rousseau, D. (2019) Recent Applications of Multispectral Imaging in Seed Phenotyping and Quality Monitoring-An Overview, *Sensors (Basel),* 19(5). DOI: https://doi.org/10.3390/s19051090

Ghoussein, Y., Faour, G., Fadel, A., Haury, J., Abou-Hamdan, H. and Nicolas, H. (2023) Hyperspectral discrimination of Eichhornia crassipes covers, in the red edge and near infrared in a Mediterranean river, *Biological Invasions,* 25(11), pp. 3619-3635. DOI: https://doi.org/10.1007/s10530-023-03131-2

Hestir, E.L., Khanna, S., Andrew, M.E., Santos, M.J., Viers, J.H., Greenberg, J.A., et al. (2008) Identification of invasive vegetation using hyperspectral remote sensing in the California Delta ecosystem, *Remote Sensing of Environment,* 112(11), pp. 4034-4047. DOI: https://doi.org/10.1016/j.rse.2008.01.022

Luo, J., Duan, H., Ma, R., Jin, X., Li, F., Hu, W., et al. (2017) Mapping species of submerged aquatic vegetation with multi-seasonal satellite images and considering life history information, *International Journal of Applied Earth Observation and Geoinformation,* 57(pp. 154-165. DOI: https://doi.org/10.1016/j.jag.2016.11.007

Malik., A. (2007) Environmental challenge vis a vis opportunity: the case of water hyacinth, *Environ Int,* 33(1), pp. 122-38. DOI: https://doi.org/10.1016/j.envint.2006.08.004

McFeeters, S.K. (2012) The use of the Normalized Difference Water Index (NDWI) in the delineation of open water features, *International Journal of Remote Sensing,* 17(7), pp. 1425-1432. DOI: https://doi.org/10.1080/01431169608948714

Mouta, N., Silva, R., Pinto, E.M., Vaz, A.S., Alonso, J.M., Gonçalves, J.F., et al. (2023) Sentinel-2 Time Series and Classifier Fusion to Map an Aquatic Invasive Plant Species along a River—The Case of Water-Hyacinth, *Remote Sensing,* 15(13). DOI: https://doi.org/10.3390/rs15133248

Mqingwana, P., Shoko, C., Gxokwe, S. and Dube, T. (2024) Monitoring and assessing the effectiveness of the biological control implemented to address the invasion of water hyacinth (Eichhornia crassipes) in Hartbeespoort Dam, South Africa, *Remote Sensing Applications: Society and Environment,* 36(DOI: https://doi.org/10.1016/j.rsase.2024.101295

Otsu, N. (1979) A Tlreshold Selection Method from Gray-Level Histograms, *IEEE Transactions on Systems, Man, and Cybernetics,* 9(1), pp. 62-66. DOI: https://doi.org/10.1109/TSMC.1979.4310076

Paulino, R.S., Martins, V.S., Novo, E.M.L.M., Barbosa, C.C.F., Maciel, D.A., Wanderley, R.L.d.N., et al. (2025) Generation of robust 10-m Sentinel-2/3 synthetic aquatic reflectance bands over inland waters, *Remote Sensing of Environment,* 318(DOI: https://doi.org/10.1016/j.rse.2024.114593

Pimentel, D., McNair, S., Janecka, J., Wightman, J., Simmonds, C., O'Connell, C., et al. (2001) Economic and environmental threats of alien plant, animal, and microbe invasion, *Agriculture, Ecosystems and Environment,* 84(1), pp. 1-20.

Pyšek, P. and Richardson, D.M. (2010) Invasive Species, Environmental Change and Management, and Health, *Annual Review of Environment and Resources,* 35(1), pp. 25-55. DOI: https://doi.org/10.1146/annurev-environ-033009-095548

Rouse, J.W., Haas, R.H., Schell, J.A. and Deering, D.W. (1974) Monitoring the Vernal Advancement and Retrogradation (Green Wave Effect) of Natural Vegetation pp. 371.

Sabat-Tomala, A., Raczko, E. and Zagajewski, B. (2024) Airborne Hyperspectral Images and Machine Learning Algorithms for the Identification of Lupine Invasive Species in Natura 2000 Meadows, *Remote Sensing,* 16(3). DOI: https://doi.org/10.3390/rs16030580

Shekede, M.D., Kusangaya, S. and Schmidt, K. (2008) Spatio-temporal variations of aquatic weeds abundance and coverage in Lake Chivero, Zimbabwe, *Physics and Chemistry of the Earth, Parts A/B/C,* 33(8-13), pp. 714-721. DOI: https://doi.org/10.1016/j.pce.2008.06.052

Sims, D.A. and Gamon, J.A. (2003) Estimation of vegetation water content and photosynthetic tissue area from spectral reflectance: a comparison of indices based on liquid water and chlorophyll absorption features, *Remote Sensing of Environment,* 84(4), pp. 526-537. DOI: https://doi.org/10.1016/s0034-4257(02)00151-7

Singh, G., Reynolds, C., Byrne, M. and Rosman, B. (2020) A Remote Sensing Method to Monitor Water, Aquatic Vegetation, and Invasive Water Hyacinth at National Extents, *Remote Sensing,* 12(24). DOI: https://doi.org/10.3390/rs12244021

Wilcove, D.S., Rothstein, D., Dubow, J., Phillips, A. and Elizabe. (1998) Quantifying Threats to Imperiled Species in the United States: Assessing the relative importance of habitat destruction, alien species, pollution, overexploitation, and disease, *BioScience,* 48(8), pp. 607–615. DOI: https://doi.org/10.2307/1313420

Woźniak, E., Rybicki, M., Kofman, W., Aleksandrowicz, S., Wojtkowski, C., Lewiński, S., et al. (2022) Multi-temporal phenological indices derived from time series Sentinel-1 images to country-wide crop classification, *International Journal of Applied Earth Observation and Geoinformation,* 107(DOI: https://doi.org/10.1016/j.jag.2022.102683

Xing, F., An, R., Guo, X. and Shen, X. (2024) Mapping invasive noxious weed species in the alpine grassland ecosystems using very high spatial resolution UAV hyperspectral imagery and a novel deep learning model, *GIScience & Remote Sensing,* 61(1). DOI: https://doi.org/10.1080/15481603.2024.2327146

Xu, H. (2007) Modification of normalised difference water index (NDWI) to enhance open water features in remotely sensed imagery, *International Journal of Remote Sensing,* 27(14), pp. 3025-3033. DOI: https://doi.org/10.1080/01431160600589179

Li, S., & Wu, Y. (2025). A multi-temporal image differencing approach [Data set]. Zenodo. https://doi.org/10.5281/zenodo.17368419